The Use of Multiresolution Analysis and Wavelets Transform for Merging SPOT Panchromatic and Multispectral Image Data

Bruno Garguet-Duport, Jacky Girel, Jean-Marc Chassery, and Guy Pautou

Abstract

Several techniques have been developed to merge SPOT 10-m resolution panchromatic data (SPOT P) with simultaneously acquired 20-m resolution multispectral data (SPOT XS). Normally, the objective of these procedures is to create a composite image of enhanced interpretability. The current merging methods may not be satisfying; they can distort the spectral characteristics of the XS images and, as a result, the analysis becomes difficult. In this paper a method allowing the use of 10-m resolution XS data while conserving the spectral properties of the original 20-m data is presented. This method uses a multiresolution analysis procedure based upon the wavelets transform; it is applied to remotely sensed SPOT P and SPOT XS images of the river junction Arc-Isère (France). This new method is compared with the IHS method and P+XS method. The wavelets method is the one which least distorts the spectral characteristics of the data. The distortions are minimal and difficult to detect.

Introduction

The objective of the improved image merging method is to generate hybrid high resolution multispectral images that attempt to preserve the radiometric characteristics of the original multispectral data. This is very important for our group because we are mostly interested in vegetation analysis.

A number of methods for merging panchromatic images with multispectral images are known from literature. Pradines (1986) proposed a method for merging four SPOT panchromatic pixels with a corresponding SPOT XS pixel. Price (1987) used merging methods for display techniques. Three merging methods have been compared (Chavez *et al.*, 1991) and no example was found to be well adapted to vegetation analysis. The most common procedure was the Intensity-Hue-Saturation (IHS) method which has been used by Carper *et al.* (1990), Chavez *et al.* (1991), and Ehlers (1991). For example, recently Pellemans *et al.* (1993) have demonstrated that the IHS method was not adapted to vegetation, and they proposed a method based on the sensors radiometric properties.

It is desirable that any procedure for merging high resolution panchromatic data with low resolution multispectral data should preserve the original spectral characteristics of the latter as much as possible. The procedure should be optimal in the sense that only the additional spatial information available in higher resolution data is imported into the multispectral bands.

The purpose of the present study was to present a 10-m simulated method for XS images while conserving spectral properties of original XS 20-m images. This method uses two tools coming from the signal processing field, based on solid mathematical procedures: multiresolution analysis and the wavelet transform. This new merging method was compared with the most common merging procedures such as IHS (Carper *et al.*, 1990; Kay, 1990) and P+XS (Anonymous, 1986).

Multiresolution Analysis and Wavelet Transform

The Wavelet Transform

Multiresolution analysis based on wavelets theory permits the introduction of the concept of details between successive levels of scale or resolution.

To define the wavelet transform (Meyer, 1992), it is necessary to introduce a function $\Psi(t)$ called the generating wavelet. Such a function $\Psi(t)$ is mainly concentrated near 0 and is characterized by a rapid decrease when $|t|$ increases. We say that $\Psi(t)$ is well localized (Mallat, 1989). Moreover, $\Psi(t)$ has to be oscillant in order to present a good localization in the frequency domain.

This condition was expressed by the equation

$$\int_{-\infty}^{+\infty} \Psi(t)dt = \ldots \int_{-\infty}^{+\infty} t^{m-1}\Psi(t)dt = 0. \quad (1)$$

The generating wavelet allowed the introduction of wavelet $\Psi_{(a,b)}(t)$ depending on two parameters: a scale factor a and a translation factor b: i.e.,

$$\Psi_{(a,b)}(t) = \frac{1}{\sqrt{a}}\,\Psi\left(\frac{t-b}{a}\right),\ a > 0,\ b \in R \quad (2)$$

Grossmann and Morlet have proved that, under this condi-

B. Garguet-Duport is with the Centre de Biologie Alpine, Laboratoire Hydrosystèmes Alpins, BP 53 38041, Grenoble cedex 9, and TIMC-IMAG Institut Albert Bonniot Domaine de la Merci 38706 La Tronche Cedex.

J. Girel is with the Centre de Biologie Alpine, Laboratoire Hydrosystèmes Alpins, BP 53 38041, Grenoble cedex 9, and CNRS URA 1451, Ecologie des eaux douces et des grands fleuves (Lyon I).

J.-M. Chassery is with the TIMC-IMAG Institut Albert Bonniot Domaine de la Merci 38706 La Tronche Cedex.

G. Pautou is with the Centre de Biologie Alpine, Laboratoire Hydrosystèmes Alpins, BP 53 38041, Grenoble cedex 9.

Photogrammetric Engineering & Remote Sensing, Vol. 62, No. 9, September 1996, pp. 1057–1066.

0099-1112/96/6209-1057$3.00/0

TABLE 1. COEFFICIENTS OF THE FILTERS ASSOCIATED WITH THE 5 BY 7 WAVELET USED.

5-7	n	$h(n)$	$\tilde{h}(n)$
	−3		−3/280
	−2	−1/20	−3/50
	−1	1/4	73/280
	0	−3/5	17/20
	1	1/4	73/280
	2	1/20	−3/56
	3		−3/280

tion for $\Psi(t)$ to be real, such a set of functions $\Psi_{(a,b)}(t)$ can be used as an orthogonal base of square bounded functions.

Thus, each signal $f(t)$ can be expressed in the basis, and the corresponding coefficients are defined as wavelets coefficients of $f(t)$ and expressed by the scalar product

$$\int_{-\infty}^{+\infty} f(t)\Psi_{(a,b)}(t)dt \tag{3}$$

Such coefficients correspond to the fluctuation of the signal $f(t)$ near the point b and the scale a. This coding has the advantage of representing a function at different levels of scale. At each level we obtain notions of details corresponding to information belonging to this level with regard to the previous one. We can organize the signal/image information as a sequence of detail appearing at different levels of resolution.

We used the biorthogonal approach of wavelet decomposition, from one level to the next one successively. We used a filtering method followed by subsampling (Mallat, 1989). This image was decomposed in a low frequency version and three images of details which corresponded to the three directions: horizontal, vertical, and diagonal.

It was also important to mention the reversibility of this transform in order to reconstruct the image at the initial resolution without losing any detail information.

Implementation

To be clear and simple, we have chosen to present the implementation of the wavelets transform in the case of a mono-dimensional signal. We will then easily deduce from it the case of the bi-dimensional signal. To implement the transform, we did not use the scale function Φ and its associated wavelet Ψ directely, but h and g filters as well as the corresponding mirror filters. The properties of these filters can be deduced from those of the wavelets and the scale function. The h filter associated with Φ is a low-pass filter, while the g filter which is associated with the wavelet is a high-pass filter Ψ (Table 1). The principles of the analysis stage and synthesis stage are successively presented below.

The Analysis Stage

Let S^0 be the initial signal, that is to say, the full resolution. An approximation S^1 of this signal has to be obtained from S^0, which is possible due to a convolution of S^0 with the low-pass filter deduced from the scale function associated to the wavelet (Figure 1). The resulting S^1 was a smoothed or debased version of S^0.

The difference between S^1 and S^0, denoted D^1, corresponded to the details of the S^0 resolution. This difference was obtained with a high-pass filter deduced from the wavelet. If S^0 had N samples, then the signals S^1 and D^1 will both have $N/2$ samples. This comes from the resolution factor which is 2 and corresponds to the undersampling factor. This can be expessed as follows:

Let S^0 be a signal at the j resolution, h_n be the low-pass filter, and g_n be the high-pass filter. Then, the approximation at S^{j+1} resolution and the details called D^j can be obtained according to the following formulas:

$$\begin{aligned} S_n^{j+1} &= \sum_k h_{(2n-k)} S_k^j \\ D_n^{j+1} &= \sum g_{(2n-k)} S_k^j \end{aligned} \tag{4}$$

For the bi-dimensional case, the image was considered as a vector matrix and Equation 4 was applied to all the lines and all the columns successively according to direction (A) as shown in Figure 1.

In that way, four under images (*HH*, *GH*, *HG*, and *GG*) were obtained from one full resolution image. *HH* was the context image at the inferior resolution, *GH* was the image of the horizontal details, *HG* was the image of the vertical details, and *GG* was the image of the diagonal details.

Synthesis Stage

In the case of the mono-dimensional signal, this stage consisted of reconstructing S^0 from S^1 and D^1. The signal S^j with the j resolution was obtained using the following formula:

$$S_n^j = 2\sum_k h_{(n-2k)} S_k^{j+1} + \sum_k g_{(n-2k)} D_k^{j+1} \tag{5}$$

where S^{j+1} is the signal at $j+1$ resolution and D^{j+1} are the details associated with the j resolution.

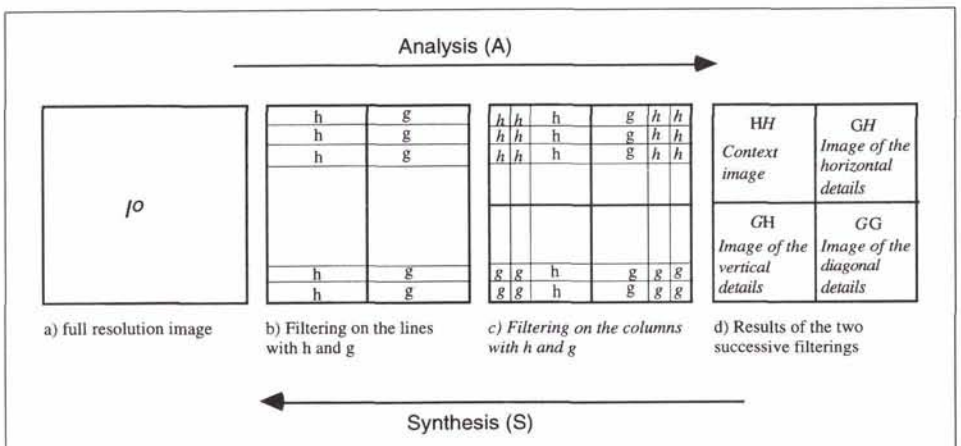

Figure 1. General diagram of the implementation. h and g: filters for the lines; *h* and *g*: filters for the columns.

In the case of the bi-dimensional signal, the original image S^0 had to be obtained from the context image HH, and the details images HG, GH, and GG. The reconstruction formula (Equation 5) is applied first to all the lines and second to all the columns according to the direction S shown in Figure 1. This reconstruction is possible due to the wavelets transform reversibility and the exact reconstruction property of the associated filters.

The multiresolution analysis and the wavelets transform already have some applications in image processing and remote sensing: e.g., compression (Antonini *et al.*, 1992), speckle processing in SAR imagery (Ranchin, 1993), rectification (Djamdji, 1993; Djamdji *et al.*, 1993), and segmentation (Fau *et al.*, 1993). For merging images with different spatial resolutions, some results have already been obtained by Mangolini *et al.*, 1993).

Data Acquisition and Study Areas

The SPOT data were collected on 21 July 1990 by SPOT (Satellite Pour l'Observation de la Terre). It is a SPOT XS and SPOT P image (Plate 1) of the river junction "Arc-Isère" near Albertville (Olympic City), France (Figure 2).

The Arc and Isère rivers were diked during the 19th century and, as a result, their stream corridors were changed by important disturbances which markedly transformed the riparian landscape. More recently, channelized beds were affected by entrenchment processes which caused perturbations such as the lowering of the superficial water table in the channels and under the adjacent bottomlands. These perturbations could initiate major changes in plant communities and farmed areas.

The Isère/Arc junction is considered an interesting study area because it is a mosaic of habitats, including

- wetlands on fine deposits;
- bare soils, dry meadows, and brushwoods on coarse deposits;
- farmed zones with various yields;
- populus *sp* cultivations;
- old and recent gravel-mining ponds; and
- urban space.

Remote sensing appears to be the most sustainable tool allowing the analysis of the ecological landscape variations over space and time.

Wavelets Merging Methods

Merging information from different imaging sensors involves two distinct steps (Chavez and Bowell, 1988). First, the digital images from both sensors were geometrically registered to one another. Next, the information contents—both spatial and spectral—were mixed to generate a single data set that contained the best of both sets.

First, the SPOT XS and SPOT P images were geometrically corrected in order to be superimposed. This was done using image modeling processes and the constitution of a digital elevation model (Novak, 1992) of the study area. Next, two steps are necessary (Figure 3) for the wavelet merging method (Garguet-Duport *et al.*, 1994a):

- Having produced three new SPOT panchromatic images whose histograms are specified according to the histogram of each SPOT XS band, the first step consists in extracting (from the three panchromatic images' information content) the structures (also called "details") present between the 10-m and 20-m spatial resolutions (Figure 4). These structures are isolated into three wavelet coefficients which correspond to the detail image according to the three directions (vertical, horizontal, and diagonal). Each set of three detail images extracted from one panchromatic image corresponds to the spatial information, at 10-m, for one SPOT XS band.
- The second step consisted of introducting these details into each XS-band through the inverse wavelet transform (Figure 5). Thus, at 10 m of resolution, simulated images are produced. The spectral information content of original XS images was conserved because only the scale structures between 10-m and 20-m resolutions have been added.

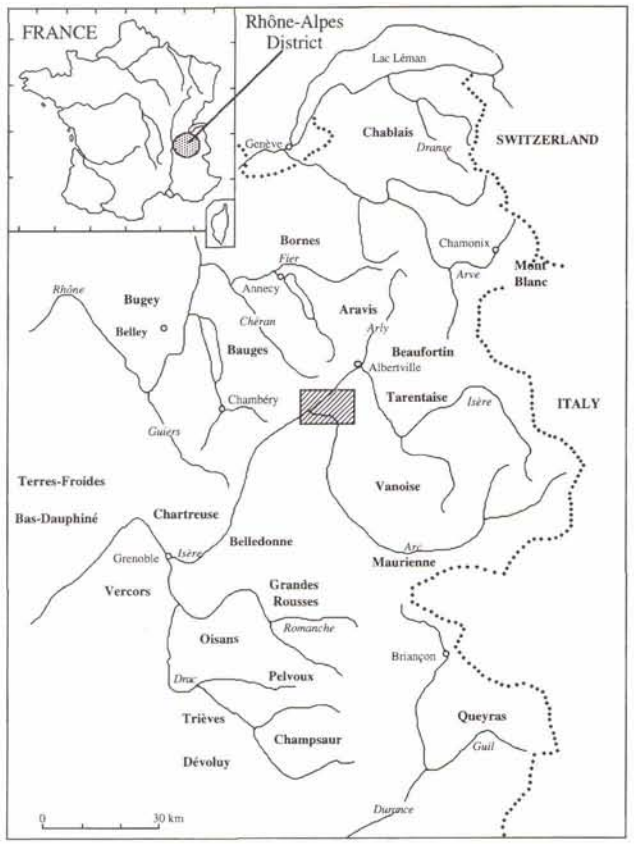

Figure 2. Location of the area studied.

Results and Discussion

To interpret the performances of this new merging method, we have considered three criteria.

Geometrical Improvement

Because we do not have any XS image at a 10-m resolution to compare with, the evaluation of the geometrical improvement poses a problem. To avoid it, we applied the merging method at an inferior level of resolution, that is to say, on a SPOT panchromatic image at a 20-m resolution and a SPOT XS image at a 40-m resolution. This merging method allowed us to simulate an XS image at a 20-m resolution by using the scale structures between the 40- and 20-m resolution of the image. This image was compared with the SPOT XS image of origin in order to evaluate the geometric improvement.

The results are shown in Plate 2. Here, we can see that the XS image simulated at a 20-m resolution (Plate 2b) and the XS image of origin (Plate 2a) do not show any difference. The luminance histograms of both images have the same general shape, with a light compression of the radiometric values for the XS image simulated at a 20-m resolution. However, this compression was not perceptible, visually speaking. The difference between the two XS images (Plate 2e) did not show any particular structure, which indicated that the scale structures between 40 and 20 m resolution have really been injected in the XS image simulated at 20 m.

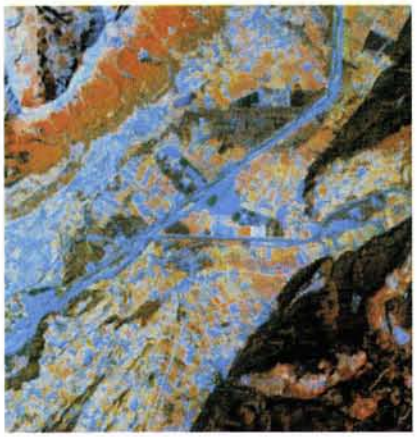

(a)

(b)

Plate 1. SPOT HRV image of the "Arc-Isère" river junction, France, recorded on 21 July 1990 (© SPOT Image Copyright 1990 CNES). (a) Original image in the color composite of the XS bands 3, 2, 1 as red, green, and blue, respectively. The spatial resolution is 20 m, and 512 by 512 pixels are shown. (b) Original image in the panchromatic band. The spatial resolution is 10 m, and 1024 by 1024 pixels are shown.

Preservation of the Spectral Characteristics

We compared the radiometric values stemming from different merging methods and the original 20-m XS image. The following merging methods were compared with the wavelet method: the IHS method (Carper *et al.*, 1990; Kay, 1990) and the P+XS method (Anonymous, 1986). These two methods are currently used in ecological framework studies.

Because the XS images of origin at a 20-m resolution and

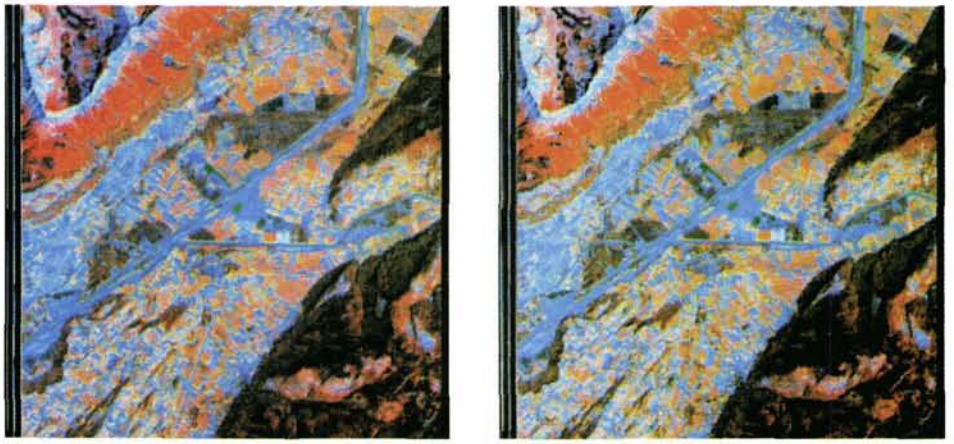

(a) (b)

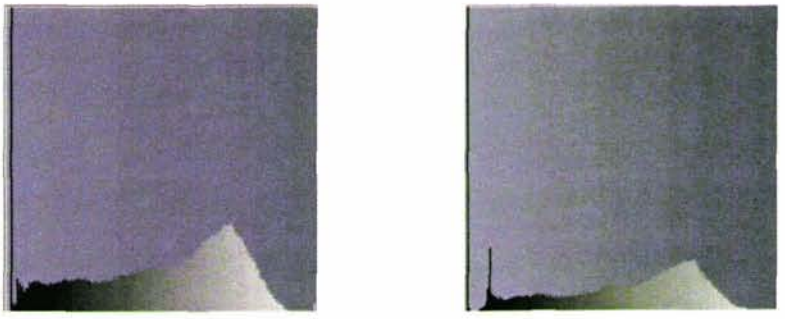

(c) (d)

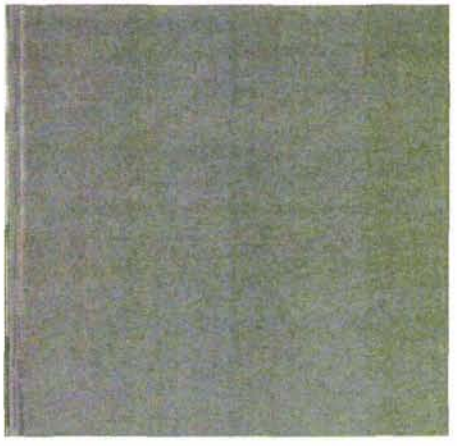

(e)

Plate 2. Checking of the merging method principle. (a) Color composite of the original XS image at 20 m resolution. (b) Color composite of the SPOT XS image reconstructed by the wavelets merging method. (c) and (d) are histograms of (a) and (b), respectively. (e) Image of the difference between (a) and (b).

the XS merging images do not have the same size, we cannot compare their radiometry with a simple arithmetic subtraction between the two images. In order to quantify the radiometry variations produced by the merging method, we have worked out the differences between the averages and the variances for each channel (red, green, and blue) for the image of reference and the merging images. To work it out, we used the following formulas:

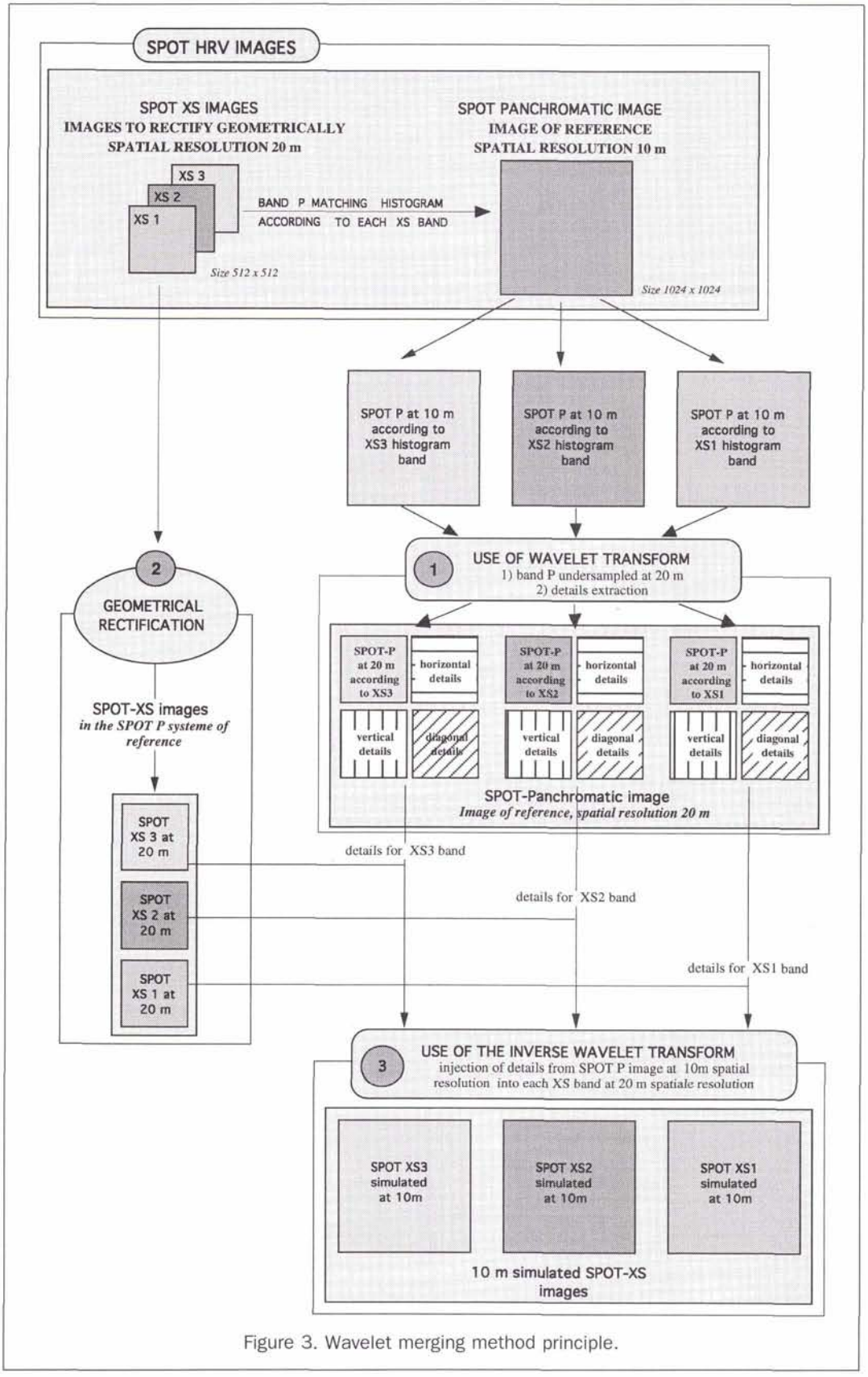

Figure 3. Wavelet merging method principle.

For the average: $\mu = \sum \left| \frac{h(i)}{N} - \frac{g(i)}{N/4} \right|$ (6) For the variance: $\delta^2 = \left| \frac{\sum (h(i) - \mu_h)^2}{N} - \frac{\sum (g(i) - \mu_g)^2}{N/4} \right|$ (7)

(a)

(b)

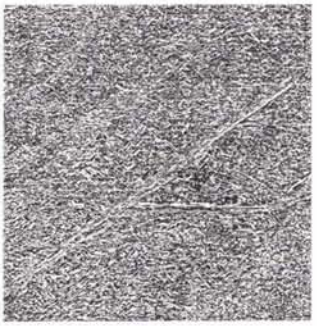

(c)

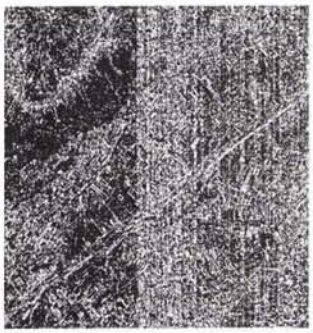

(d)

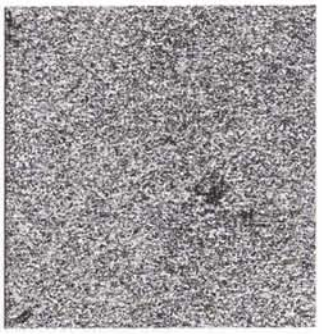

(e)

Figure 4. The first step of the wavelet merging method; example for the SPOT XS2 band (© SPOT Image Copyright 1990 CNES). (a) Panchromatic image with its histogram specified according to the SPOT XS2 histogram. The spatial resolution is 10 m, and 1024 by 1024 pixels are shown. (b) Context image with 20-m spatial resolution. (c) Image of the "horizontal structures" at 10 m resolution. (d) image of the "vertical structures" at 10 m resolution. (e) image of the "diagonal structures" at 10 m resolution. This wavelet merging method enabled us to get all the scale structures included between 10 and 20 m. This wavelet merging method is applied to three panchromatic bands, each one having its own histogram specified according to one of the XS bands.

(a)

(b)

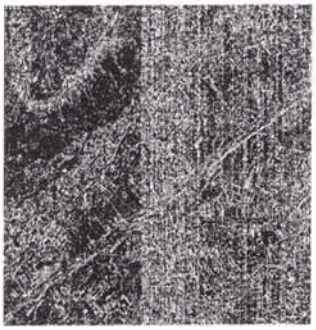

(c)

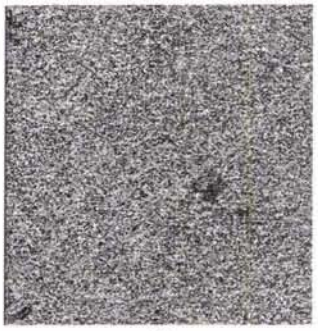

(d)

(e)

Figure 5. The second step of the wavelet merging method; simulation of the SPOT XS2 at 10 m (© SPOT Image Copyright 1990 CNES). (a) SPOT XS2 image geometrically rectified according to the SPOT panchromatic band geometry; the spatial resolution is 20 m. (b), (c), and (d) Detail images according to three directions derived from the first step of the wavelet merging method (Plate 1). The inverse wavelet method involves injecting the three detail images in the XS2 band in order to simulate an XS2 band at 10 m resolution (e).

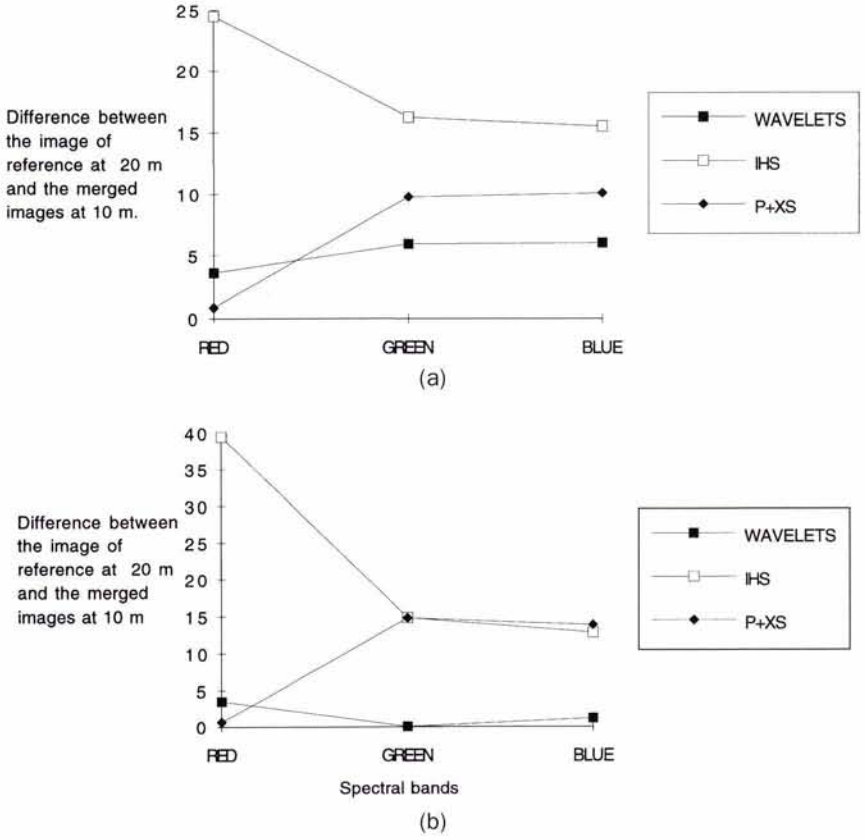

Figure 6. (a) Difference in absolute value between the averages. (b) Difference in absolute value between the variances.

where $h(i)$ is the histogram of the image of reference and $g(i)$ is the histogram of the merging image.

Figure 6 shows the results. The analysis of the radiometric characteristics proved that this method was more efficient than the classical IHS and P+XS merging methods. The wavelets method appeared to allow a better preservation of the radiometic characteristics of the original SPOT XS image.

Thematic Analysis

The results of visual inspection were performed by professional photointerpreters, specialists in vegetation mapping. In Plate 3, a color composite image, made with the XS 10-m bands, and an other one made, with the panchromatic band to enhance vegetation analysis, are shown.

For the thematic analysis, the professionnal photointerpreters used an aerial photograph taken on 22 July 1990 as a reference. They located in it 102 taxons divided into three classes: natural vegetation, farming, and urban zones. Then, they tried to find these 102 taxons in each image. Figure 7 shows the results of this analysis. The image merged by the wavelet method allows us to find, for the three classes, more taxons than with the other merging methods (IHS and P+XS) and more taxons than in each original image (SPOT XS at a 20-m resolution, SPOT P at a 10-m resolution). The color composite image that we have called "natural colors" gave the best results concerning vegetation characteristics. The wavelet method appears to be well adapted to the vegetation analysis. The images produced by this method maintains good spectral quality while preserving the high spatial panchromatic band resolution (Garguet-Duport *et al.*, 1994b).

Hence, beyond these high resolution new channels, it is possible to carry out image processing techniques (classifications, color-composite imagery, band ratioing, etc.) which have been currently used for several years. Concerning vegetation, the wavelet merging methods allowed a better automatic classification (fewer pixels mixed) than the other methods (Garguet-Duport, 1994). These numerical techniques are all the more interesting as the images concerned allowed the SPOT-XS

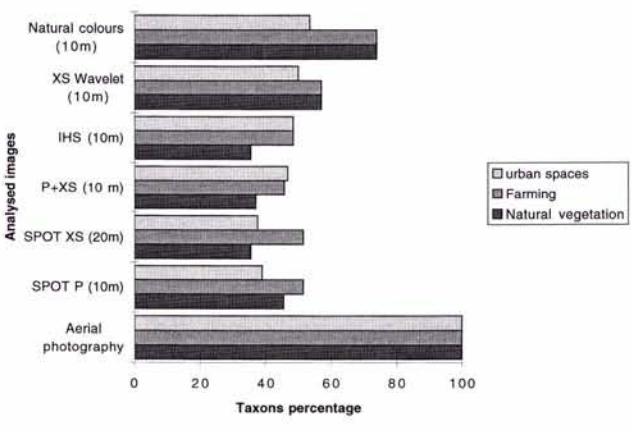

Figure 7. Thematic analysis of the images.

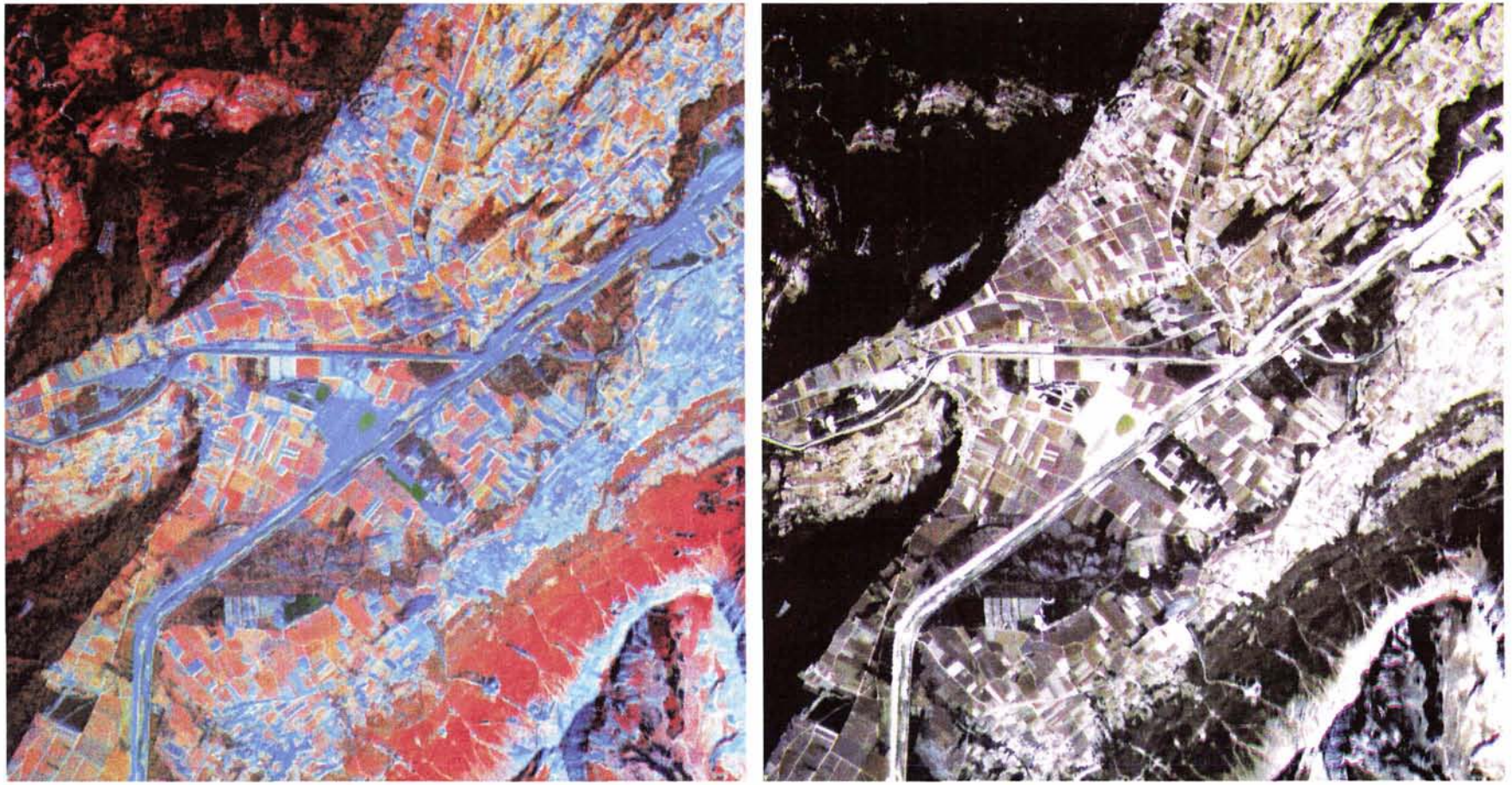

(a) (b)

Plate 3. SPOT HRV images simulated at a 10-m spatial resolution with the wavelet merging method (© SPOT Image Copyright 1990 CNES). (a) Color composite made by using the wavelet merging method of the XS bands 3, 2, and 1 as red, green, and blue, respectively. This print should be compared with Plate 1a to show that the spectral characteristics have not been made by the wavelet merging method. (b) Natural color composite image made by using the result of the ACP transformation (on the wavelet merging method XS bands) and the panchromatic band. ACP1, panchromatic and XS1 as red, green, and blue, respectively.

at a 20-m resolution to retain its radiometric characteristics while being simulated at a 10-m resolution.

Conclusions

The major advantage of the wavelet merging method is in the minimal distortion of the spectral characteristics of the data. This result could be obtained because the wavelet method has only added the scale structures contained between 10-m resolution and 20-m resolution images. Another advantage was that these scale structures (panchromatic "details") can be applied to each XS band independently.

The visual comparison indicated that the wavelet method generates results with good spatial resolution similar to the IHS method or the P+XS method.

The results stemming from this merging method are very promising. Analysis and thematic processings (i.e., production of thematic color composite images, automatic classification) carried out from that high resolution data have exhibited a significant improvement of imagery and a great potential concerning vegetation mapping of the floodplains which needs high spatial and spectral resolutions.

References

Anonymous, 1986. *Guide des utilisateurs de données SPOT*, Editeurs CNES et SPOT Image, Toulouse, France.

Antonini, M., M. Barlaud, P. Mathieu, and I. Daubechies, 1992. Image Coding Using Wavelet Transform, *IEEE Transactions on Image Processing*, 1(2):205–220.

Carper, W.J., T.M. Lillesand, and R.W. Kiefer, 1990. The Use of Intensity-Hue-Saturation Transformation for Merging SPOT Panchromatic and Multispectral Image Data, *Photogrammetric Engineering & Remote Sensing*, 56(4):459–467.

Chavez, P.S., and J.A. Bowell, 1988. Comparison of the Spectral Information Content of Landsat Thematic Mapper and SPOT for Three Different Sites in the Phoenix, Arizona, Region, *Photogrammetric Engineering & Remote Sensing*, 54(12):1699–1708.

Chavez, P.S., S.C. Sides, and J.A. Anderson, 1991. Comparison of Three Different Methods to Merge Multi-Resolution and Multispectral Data: Landsat TM and SPOT Panchromatic, *Photogrammetric Engineering & Remote Sensing*, 57(3):295–303.

Djamdji, J.P., 1993. *Analyse en ondelettes et mise en correspondance en télédétection*, Thèse Science de l'ingénieur, Université, Nice-Sophia Antipolis.

Djamdji, J.P., A. Bijaoui, and R. Manière, 1993. Geometrical Registration of Images: The Multiresolution Approach, *Photogrammetric Engineering & Remote Sensing*, 59(5):645–653.

Ehlers, M., 1991. Multi-Sensor Image Fusion Techniques in Remote Sensing, *ISPRS Journal of Photogrammetry and Remote Sensing*, 46(3):19–30.

Fau, R., B.G. Bénier, and J. Boucher, 1993. Segmentation markovienne pyramidale d'images, *16th Symposium Canadien sur la Télédétection, 8e Congrès de l'association québéquoise de télédétection*, Sherbrooke, Québec, Canada.

Garguet-Duport, B., 1994. *Fusion d'images et télédétection en écologie du paysage. Application à l'étude structurale d'un corridor fluvial alpin*, thése informatique appliquée—Biologie, Université, Joseph Fourier Grenoble.

Garguet-Duport, B., J.-M. Chassery, J. Girel, and G. Pautou, 1994a. A New Merging Method from Multispectral and Panchromatic SPOT Images for Vegetation Mapping, *S.P.I.E The European Symposium on Satellite Remote Sensing*, Headquarters of the National Research Center of Italy Rome, Italy, S.P.I.E EUROPTO Series, 2315:625–634.

Garguet-Duport, B., J. Girel, and G. Pautou, 1994b. Analyse spatiale d'une zone alluviale par une nouvelle méthode de fusion d'images SPOT multispectrale (XS) et SPOT panchromatique (P), *Comptes Rendus de l'Academie des Sciences, Série III Life Science*, 317(2):194–201.

Kay, S., 1990. *HSI Color Image Processing Techniques and Applications*, Data Translation Inc.

Mallat, S.G., 1989. A Theory for Multiresolution Signal Decomposition: The Wavelet Representation, *IEEE transactions on Pattern Analysis and Machine Intelligence*, 11(7):674–693.

Mangolini, M., T. Ranchin, and L. Wald, 1993. Fusion d'images SPOT multispectrale (XS) et panchromatique (P), et d'image radar, *De l'optique au radar, les applications de SPOT et ERS, CNES Ceradués Editions*, Paris, pp. 199–209.

Meyer, Y., 1992. *LES ONDELETTES: Algotihmes et Applications*, Armand Colin, Paris.

Novak, K., 1992. Rectification of Digital Imagery, *Photogrammetric Engineering & Remote Sensing*, 58(3):339–344.

Pellemans, A.H.J.M., R.W.L. Jordans, and R. Allewiijn, 1993. Merging Multispectral and Panchromatic SPOT Images with Respect to the Radiometric Properties of the Sensor, *Photogrammetric Engineering & Remote Sensing*, 59(1):81–87.

Pradines, D., 1986. Improving SPOT Images Size and Multispectral Resolution, *Proceedings of the S.P.I.E Earth Remote Sensing Using the Landsat Thematic Mapper and SPOT Systems*, 660:98–102.

Price, J.C., 1987. Combining Panchromatic and Multispectral Imagery from Dual Resolution Satellite Instruments, *Remote Sensing of Environment*, 21:119–128.

(Received 19 April 1994; revised and accepted 7 April 1995; revised 25 May 1995)